Dendron-Functionalized Bis(terpyridine)-Iron(II) or -Cadmium(II) Metallomacrocycles: Synthesis, Traveling-Wave Ion-Mobility Mass Spectrometry, and Photophysical Properties

ARTICLE *in* CHEMISTRY - A EUROPEAN JOURNAL · APRIL 2011

Impact Factor: 5.73 · DOI: 10.1002/chem.201003681 · Source: PubMed

7 AUTHORS, INCLUDING:

Xiaopeng Li
University of Akron
44 PUBLICATIONS **1,029** CITATIONS
SEE PROFILE

Xiaocun Lu
University of Akron
16 PUBLICATIONS **215** CITATIONS
SEE PROFILE

Chrys Wesdemiotis
University of Akron
259 PUBLICATIONS **5,661** CITATIONS
SEE PROFILE

George Richard Newkome
University of Akron
497 PUBLICATIONS **12,659** CITATIONS
SEE PROFILE

CHEMISTRY
A EUROPEAN JOURNAL

DOI: 10.1002/chem.201003681

VIP

Dendron-Functionalized Bis(terpyridine)–Iron(II) or –Cadmium(II) Metallomacrocycles: Synthesis, Traveling-Wave Ion-Mobility Mass Spectrometry, and Photophysical Properties

Jin-Liang Wang,[a] Xiaopeng Li,[b] Xiaocun Lu,[a] Yi-Tsu Chan,[a] Charles N. Moorefield,[a] Chrys Wesdemiotis,*[a, b] and George R. Newkome*[a, b]

Abstract: The synthesis, purification, structural analysis, and photophysical properties of a series of five-, six-, and seven-sided Fe^{II} macrocycles and the corresponding hexameric Cd^{II} macrocycle, all prepared by self-assembly of a 120° bis(terpyridine) ligand modified with first- and second-generation 1→3 *C*-branched dendrons, are reported. All metallomacrocycles were fully characterized by ^{1}H and ^{13}C NMR spectroscopy, traveling-wave ion-mobility mass spectrometry (TWIM MS), molecular modeling, UV/Vis absorption spectroscopy, photoluminescence, and cyclic voltammetry. A gradual increase of the collision cross sections of the Fe^{II} metallomacrocycles was observed with a successive increase of the number and molecular size of the ligands. The combination of ion-mobility mass spectrometry and NMR techniques unveils structural features that agree well with calculations. Extinction coefficients and emission are significantly modulated by increasing the ring size and changing the metal ion center from Fe^{II} to Cd^{II}.

Keywords: dendrons · macrocycles · mass spectrometry · metallocycles · self-assembly · terpyridine

Introduction

The design and synthesis of highly ordered, macromolecular architectures through self-assembly strategies are of particular interest from various supramolecular perspectives.[1] One notable strategy relies on ligand–metal–ligand coordination to construct predesigned architectures.[2–5] This approach offers a variety of opportunities for the preparation of interesting metallomacrocyclic architectures, including triangular, rectangular, pentagonal, and hexagonal shapes.[6] Aromatic N-heterocycles, especially 2,2′:6′,2″-terpyridine (tpy), play a prominent role in this protocol due to their strong binding to transition-metal ions and wide variety and positioning of tailored connectors and spacers, which enable the preparation of multinuclear derivatives.[7] Meanwhile, dendronized polymers have become an important part of supramolecular chemistry due to promising applications in, inter alia, unimolecular micelles, drug delivery, and catalysis.[8] For example, dendritic folate rosettes have been used as ion channels in liquid bilayers, which showed interesting results in the mechanism of ion transportation in biological processes.[8c] Very few examples concerning the integration of dendronized chromophores into larger metallomacrocyclic complexes through self-assembly have been reported, owing to difficulties in the synthesis and separation of the desired product from isomers or similar by-products.[9] The characterization of such large macrocycles is also a challenge due to the difficulty in obtaining single crystals of complex macrostructures. A common alternative relies on the combination of NMR spectroscopy and electrospray ionization (ESI) or matrix-assisted laser desorption ionization (MALDI) mass spectrometry (MS).[10] For example, Lin et al. reported a series of molecular polygons, as confirmed by NMR spectroscopy and MALDI MS;[11] however, for some labile species with ⟨tpy-Cd^{II}-tpy⟩ or ⟨tpy-Fe^{II}-tpy⟩ connectivity, ESI and MALDI MS can easily generate a number of differently charged complexes and/or many fragments, which significantly increases the challenge of structure verification.[12]

Drift-cell ion-mobility spectrometry/mass spectrometry (IMS MS)[13] or traveling-wave ion-mobility mass spectrometry (TWIM MS)[14] offers a solution to this problem, because they afford dispersion based on the shape and charge state; with this capability, fragment and intact-assembly peaks of the same mass-to-charge ratio (*m/z*) as well as isomeric architectures of the same assembly can be deconvoluted.[15] The time needed for an ion to travel through the ion-mobility region is defined as its drift time; from this time, which is affected by the mass, charge, and ion shape, the collision

[a] Dr. J.-L. Wang, X. Lu, Dr. Y.-T. Chan, Dr. C. N. Moorefield, Prof. Dr. C. Wesdemiotis, Prof. Dr. G. R. Newkome
Departments of Polymer Science
The University of Akron, 302 Buchtel Common
Akron, OH, 44325 (USA)
Fax: (+1) 330-972-2368
E-mail: newkome@uakron.edu

[b] Dr. X. Li, Prof. Dr. C. Wesdemiotis, Prof. Dr. G. R. Newkome
Department of Chemistry, The University of Akron
302 Buchtel Common, Akron, OH, 44325 (USA)
Fax: (+1) 330-972-6085
E-mail: wesdemiotis@uakron.edu

Supporting information for this article is available on the WWW under http://dx.doi.org/10.1002/chem.201003681.

cross section of the traveling ion can be derived.[15d,e] For comparison, the collision cross sections of individual architectures or conformations can also be calculated by molecular modeling simulations.[15d,e] Comparison of experimental collision cross-sectional data with calculated values affords information about the conformation and geometry of the drifting ions.[15d,e]

Herein, we present the one-pot synthesis, isolation, and structural characterization of a family of metallomacrocycles ranging from pentamer to heptamer possessing ⟨tpy-Fe^{II}-tpy⟩ or ⟨tpy-Cd^{II}-tpy⟩ connectivity. These metallocycles were obtained from bis(terpyridine) ligands possessing a predesigned 120° angle between the two terpyridine moieties as well as either first- or second-generation (G1 or G2, respectively) dendron. Investigation of these macromolecules by NMR spectroscopy, TWIM MS, UV/Vis absorption spectroscopy, photoluminescence, molecular modeling, and cyclic voltammetry provides information about their molecular size and shape, as well as their photophysical and electrochemical properties, while keeping a common metallomacrocyclic backbone with similar ligands and metal ion centers. The cross-sectional data, acquired with TWIM MS and molecular modeling, reveal detailed snapshots of the conformational space traversed by the dendron-based macrocycles.

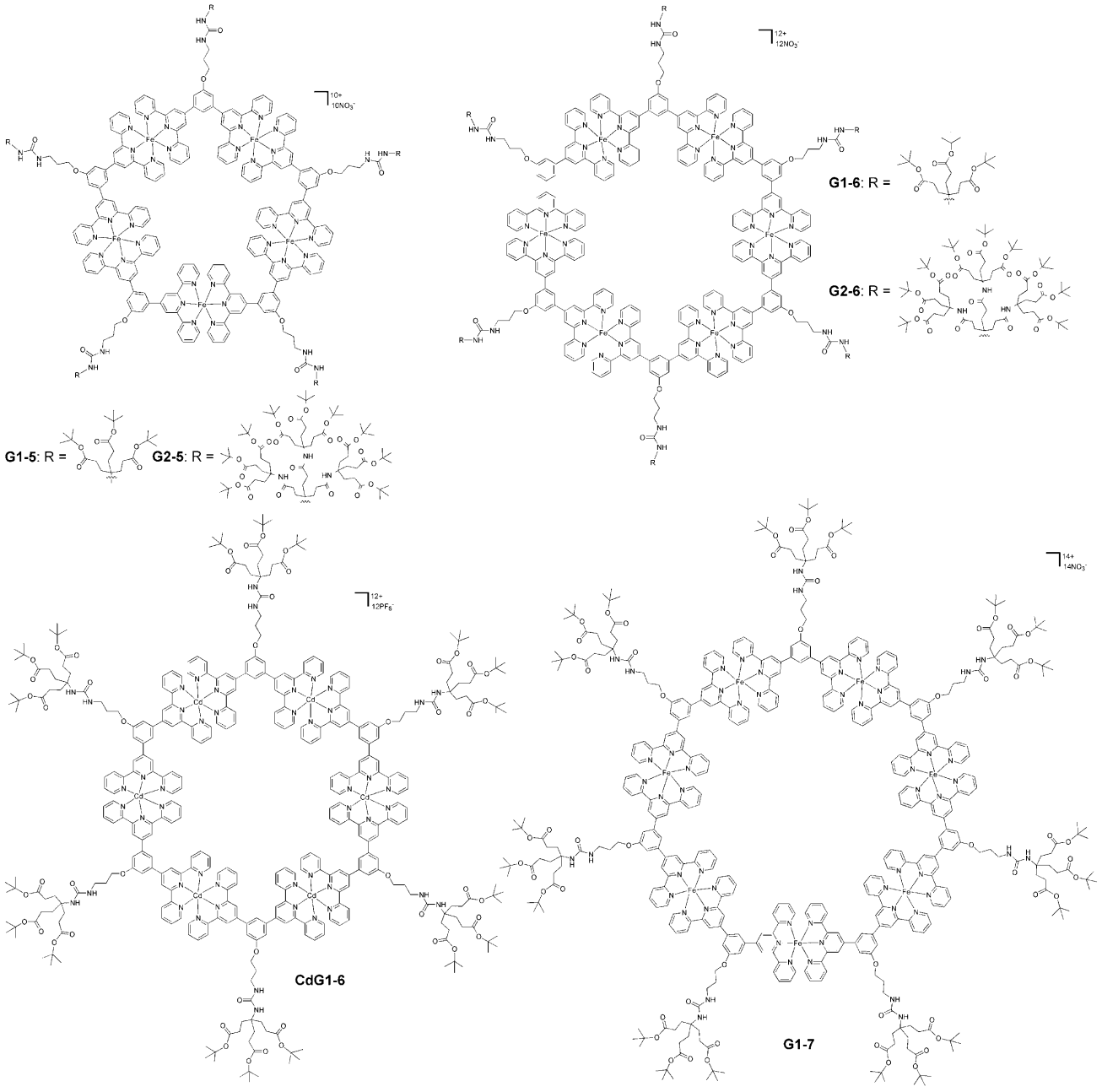

Results and Discussion

Scheme 1 illustrates the synthetic approach, which employs urea connectivity to 1→3 *C* branched, G1 and G2 dendrons carrying the bis(terpyridine) ligand moieties **G1tpy** or **G2tpy**. Treatment of the isocyanate of dendrons **2** and **3**

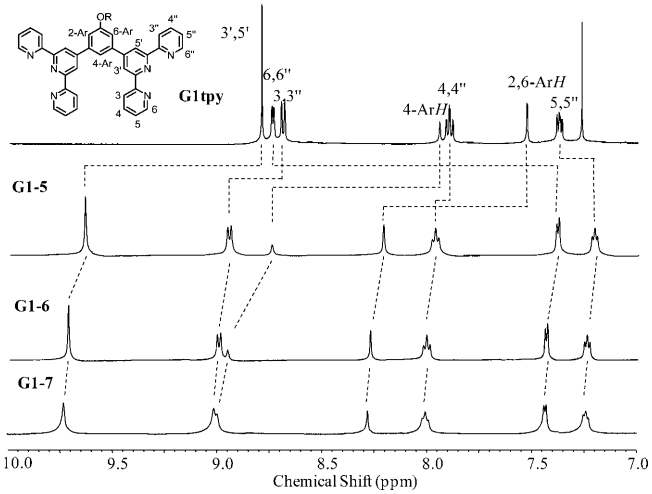

Figure 1. Aromatic regions of the 500 MHz ^{1}H NMR spectra for ligand **G1tpy** (in $CDCl_3$) and pentamer **G1-5** to heptamer **G1-7** with NO_3^- as the counterion (in CD_3OD).

with the free amine of bis(terpyridine) **1** gave **G1tpy** and **G2tpy** in 82[16] and 72% yields, respectively. The ^{1}H NMR spectrum of **G2tpy** exhibits a singlet at 8.76 ppm for the 3′,5′-tpy*H* protons and possesses a ratio of aliphatic to aromatic protons that agrees with the expected structure (see Supporting Information). The corresponding MALDI MS shows a sharp $[M+Na]^+$ molecular ion peak at $m/z=$ 2100.5, corroborating the molecular identity of the ligand **G2tpy**. A similar analysis was performed for **G1tpy** and confirmed its structure.

Treatment of **G1tpy** (Scheme 1) with 1.05 equivalents of $FeCl_2{\cdot}4H_2O$ in MeOH at 25°C for 12 h gave the pentamer **G1-5** (8%), hexamer **G1-6** (21%), heptamer **G1-7** (5%), as well as minor components that could not be isolated in pure form presumably consisting of larger macrocycles and a linear polymeric fraction. The ferromacrocycles were separated by silica-gel column chromatography, using a H_2O/MeCN/sat. KNO_3(aq) mixture as the mobile phase and gradient elution [1:12:1 (v/v/v) for **G1-5**; 1:10:1 for **G1-6**; 1:8:1 for **G1-7**]. Pentamer **G2-5** and hexamer **G2-6** were obtained from **G2tpy** and $FeCl_2{\cdot}4H_2O$ in MeOH under similar conditions in 10 and 23% yield, respectively, and were also isolated by silica-gel column chromatography eluting with H_2O/MeCN/sat.KNO_3(aq) [from 1:14:1 to 1:12:1 (v/v/v)]. The heptamer or larger macrocycles were detected as very minor components.

To better understand the photophysical properties of the Fe^{II} macrocycles, the related Cd^{II} construct with the dendronized bis(terpyridine) **G1tpy** was synthesized. Because of the enhanced lability of ⟨tpy-Cd-tpy⟩ connectivity,[15a] reaction of the **G1tpy** ligand with one equivalent of $Cd(NO_3)_2{\cdot}4H_2O$ in MeOH afforded the hexameric macrocycle **CdG1-6** in nearly quantitative yield, eliminating the necessity for chromatographic separation. The **CdG1-6**$^{12+}$ $(NO_3^-)_{12}$ salt was converted to the corresponding PF_6^- salt by dissolution in MeOH and precipitation with excess NH_4PF_6.

These metallomacrocycles are readily soluble in common organic solvents, such as $CHCl_3$, MeOH, and DMSO (with Cl^- or NO_3^-, as counterion) or MeCN and acetone (with PF_6^-, as counterion). The structure and purity of these metallomacrocycles were ascertained by ^{1}H, ^{13}C, and COSY NMR spectroscopy, as well as ESI MS. The ^{1}H NMR spectra of **G1-5**, **G1-6**, and **G1-7** with NO_3^- (Figure 1) exhibit sharp, simple patterns, as expected for such symmetric structures. Compared with the free ligand, the ^{1}H NMR spectra of the complexes show an approximate 1.3 ppm upfield shift for the 6,6′′-tpy*H*s and a 0.8 ppm downfield shift for the 3′,5′-tpy*H*s. Although all Fe^{II} macrocycles exhibit a similar peak pattern for terpyridine, there are slight variations, especially for 3′,5′-tpy*H* at about 9.7 ppm, which experiences downfield shifts when the ring size is increased from pentamer to heptamer (with **G1tpy** ligands) or to hexamer (with **G2tpy** ligands). This shift indicates that the 3′,5′-tpy*H* proton is particularly sensitive to the ring size and, hence, is a key feature

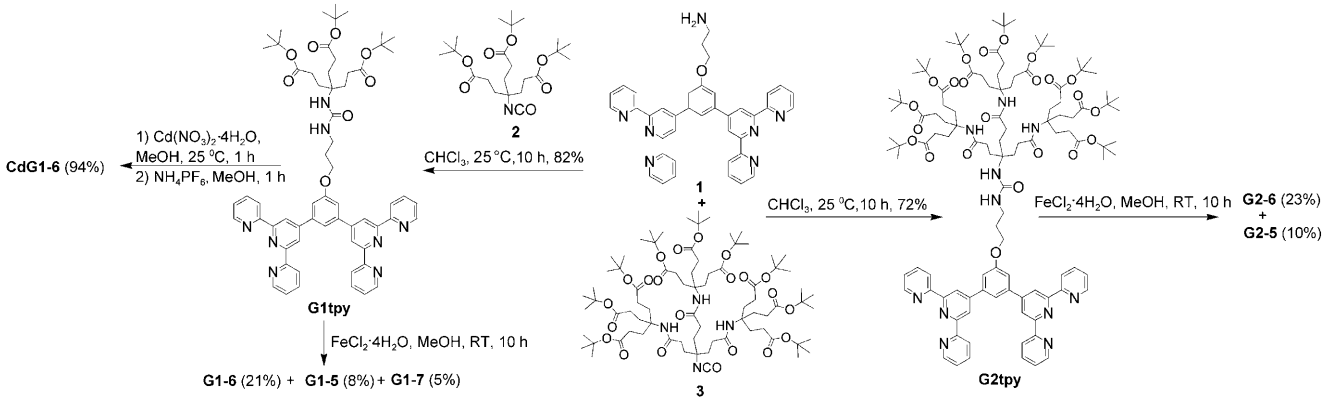

Scheme 1. Synthetic route to ligands **G1tpy** and **G2tpy** along with the self-assembled Fe^{II} or Cd^{II} metallomacrocycles.

for their structural identification. The two singlets at 8.7 and 8.2 ppm (in the spectrum of **G1-5**) are assigned to the two types of phenyl protons, namely, 4-Ar*H* and 2,6-Ar*H*, respectively. Both types show successive downfield shifts with increasing ring size; this is most noticeable for 4-Ar*H*, which shifts from 8.75 ppm in **G1-5** to 8.94 ppm in **G1-6**, and essentially merges with the 3,3″-tpy*H* peak in **G1-7**, presumably due to the enhanced crowding caused by the constricted macrocycle.[17] Further, subtle downfield shifts are observed for **G2-5** and **G2-6** in comparison with **G1-5** and **G1-6**, respectively (see Supporting Information).

The Cd^{II} hexameric complex **CdG1-6** also exhibits a sharp, symmetric pattern (^{1}H NMR spectrum; Figure S1 in the Supporting Information). The 3,3″-tpy*H*, 4,4″-tpy*H*, 5,5″-tpy*H*, and 6,6″-tpy*H* show distinct downfield shifts relative to the same protons in the Fe^{II} macrocycles **G1-6** due to the enhanced electron deficiency of the Cd^{II} metal ion center, whereas the protons belonging to 3′,5′-tpy*H*, 4-Ar*H*, and 2,6-Ar*H* exhibit upfield shifts relative to these proton in **G1-6** (PF_6^- in both complexes). The ^{1}H NMR spectrum of **CdG1-6**, which was acquired without chromatographic purification of the raw product (vide supra), affirms that the hexameric Cd^{II} macrocycle was constructed in high yield due to the lability of ⟨tpy-Cd^{II}-tpy⟩ connectivity.[7c] All ^{13}C NMR spectra of the investigated macrocycles are in full agreement with the symmetric structures (see Supporting Information).

The ESI of the Fe^{II} macrocycles with NO_3^- counterion generated a few intact macrocyclic ions along with fragments. To obtain more informative mass spectra, all NO_3^- salts were converted to the corresponding PF_6^- salts, which produce a continuous distribution of intact charge states and substantially fewer fragments upon ESI conditions,[12] as attested in Figure 2 for **G1-5** and the Supporting Information (Figures S2–S6) for the other Fe^{II} assemblies. Intact supramolecular ions carry all self-assembled metal and ligand moieties and are formed by removal of one or more of their counterions. The intact supramolecular ions observed from the synthesized complexes corroborate the expected macrocyclic structures. For example, the ESI mass spectrum of Fe^{II} macrocycle **G1-5** displays peak clusters centering at $m/z =$ 1606.7, 1256.4, 1022.8, 856.9, 730.8, 633.5, and 555.7, which have isotope spacings that correspond to charge states +4 to +10, respectively, and show isotope distributions that are in accord with those calculated for **G1-5** (Figure 2). Due to the lower stability of the ⟨tpy-Cd^{II}-tpy⟩ connectivity, relative to ⟨tpy-Fe^{II}-tpy⟩, ESI MS of the **CdG1-6** hexameric assembly leads not only to intact supramolecular peaks, centering at $m/z = 2771.2$, 2042.2, 1604.6, 1312.8, and 1104.7 and having the isotope patterns expected for charge states +3 to +7, respectively, but also to a significant number of fragments (see Supporting Information, Figure S7).

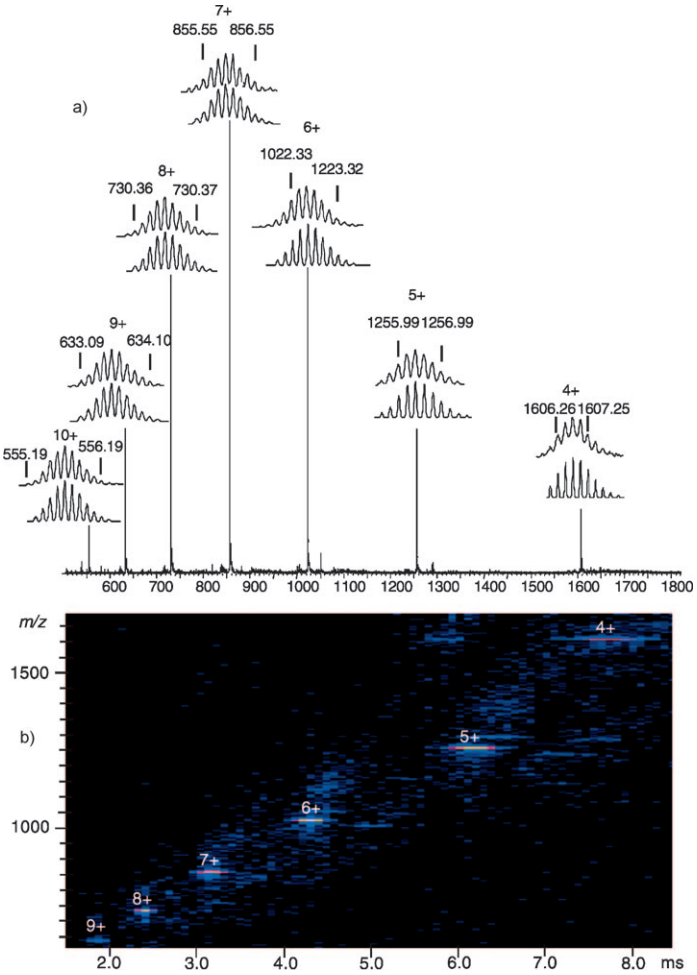

Figure 2. a) ESI mass spectrum of **G1-5**. b) Two-dimensional ESI-TWIM MS plot (*m/z* vs. drift time) of **G1-5**, acquired using a traveling-wave velocity of 350 m s^{-1} and a traveling-wave height of 8.5 V.

The absorption and emission spectra of the metallomacrocycles and corresponding bis-ligand **G1tpy** in dilute MeOH are shown in Figure 3 and summarized in Table 1. Ligand

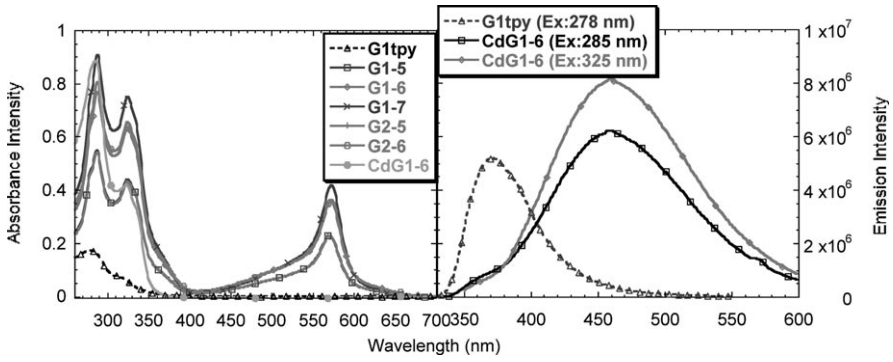

Figure 3. Absorption and emission spectra of ligand **G1tpy** and the metallomacrocycles, acquired in dilute MeOH (2.5×10^{-6} M) at 25 °C. The excitation wavelength in the emission experiments was 278 nm for **G1tpy** and 285 or 325 nm for **CdG1-6** (see insert).

Table 1. Photophysical properties of the metallomacrocycles and ligand **G1tpy** in dilute MeOH (2.5×10^{-6} M) at 25 °C.

	λ_{max} absorption [nm] ($\varepsilon\times10^{-5}$)	λ_{max} emission [nm]
G1tpy	278 (0.70), 307 (0.33)	371
G1-5	287 (2.20), 324 (1.76), 570 (0.92)	
G1-6	287 (3.08), 324 (2.55), 572 (1.44)	
G1-7	287 (3.64), 324 (3.01), 572 (1.68)	
G2-5	287 (2.18), 324 (1.73), 570 (0.92)	
G2-6	287 (3.23), 324 (2.62), 572 (1.46)	
CdG1-6	285 (3.54), 322 (1.68)	460

G1tpy exhibits ligand centered, $\pi\rightarrow\pi^*$ transitions (LC) at about 278 and 307 nm. The Fe^{II} macrocycles in dilute MeOH were purple, while the Cd^{II} analogue was colorless. Compared with the ligand, the Fe^{II} macrocycles also exhibit distinct absorption bands centered at about 570 nm, which are attributed to the metal-to-ligand charge transfer (MLCT) transition.[18] The LC absorption bands of **G1tpy** are red-shifted for the Fe^{II} macrocycles, which show distinct peaks at approximately 287 and 324 nm. Molar extinction coefficients progressively increase from pentamer **G1-5** to hexamer **G1-6** to heptamer **G1-7**, as expected from the increasing number of ligand chromophores. Increasing the dendron generation on the periphery of the complexes from **G1-6** to **G2-6** leads to nearly identical absorption bands, because the bis(terpyridine) ligand backbones remain the same and the dendron functionality would not be expected to enhance absorption. However, a slight blue shift is observed for the Cd^{II} hexamer **CdG1-6**, which gives rise to absorption peaks at about 283 and 322 nm, which are assigned to intraligand charge transfer (ILCT); no MLCT peak was detected for this complex.[19] Both the ligand as well as the Cd^{II} hexamer are fluorescent in dilute solution. The emission maximum in MeOH peaks at 371 nm for the **G1tpy** ligand, but is red-shifted to 460 nm for **CdG1-6**; the latter emission is attributed to an excited state from ILCT. Notably, excitation of **CdG1-6** at either 285 or 325 nm exclusively gives a charge-transfer band, suggesting a highly efficient intramolecular energy-transfer process.[20] Meanwhile, all Fe^{II} complexes are non-emissive, as a result of the fast relaxation of the Fe^{II}–terpyridine complex to the ground state.[21]

The electrochemical properties of these macrocycles and their corresponding ligands were investigated by cyclic voltammetry in DMF and $Ag/AgNO_3$, as reference electrode. The ligand **G1tpy** only shows irreversible reduction processes at about −1.75 V, whereas the corresponding complexes show two quasi-reversible or irreversible one-electron reduction processes that can be assigned to two one-electron reduction processes of the terpyridine units.[22] All complexes exhibit one irreversible oxidation due to the Fe^{II} or Cd^{II} centers. Relevant electrochemical data are listed in Table 2 and a representative cyclic voltammetry response, obtained from **G1-5**, is displayed in Figure 4. The potentials observed for metal-centered oxidation or terpyridine reduction are quite similar for the different macrocycles. Compared to **G1-5**, both the oxidation and reduction processes of **G2-5** or **G1-7** become more irreversible upon increasing the dendron generation and structural bulk, which may

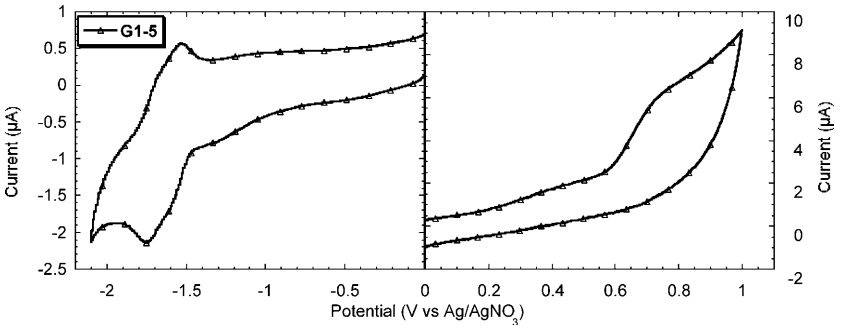

Figure 4. Cyclic voltammogram of metallomacrocycle **G1-5** in a 0.1 M solution of Bu_4NPF_6 in DMF, acquired at a scan rate of 100 mV s^{-1}.

Table 2. Electrochemical peaks, onset potentials and energy levels of metallodendrimers and ligand.[a]

	$E_{ox(peak)}$ [V]	$E_{ox(onset)}$ [V]	$E_{red(peak)}$ [V]	$E_{red(onset)}$ [V]	E_{HOMO} [eV]	E_{LUMO} [eV]	$E_{g(cv)}$ [eV]	$E_{g(opt)}$ [eV]
G1-5	0.72±0.005	0.55±0.01	−1.60±0.005 −1.74±0.005	−1.35±0.01	−5.26±0.01	−3.36±0.01	1.90±0.02	1.93±0.01
G1-6	0.70±0.005	0.50±0.01	−1.62±0.005 −1.75±0.005	−1.40±0.01	−5.21±0.01	−3.31±0.01	1.90±0.02	1.91±0.01
G1-7	–	0.51±0.01	−1.59±0.005 −1.70±0.005	−1.42±0.01	−5.22±0.01	−3.29±0.01	1.93±0.02	1.90±0.01
G2-5	-	0.55±0.01	−1.60±0.005 −1.73±0.005	−1.40±0.01	−5.26±0.01	−3.31±0.01	1.95±0.02	1.93±0.01
G2-6	–	0.51±0.01	−1.64±0.005 −1.76±0.005	−1.46±0.01	−5.22±0.01	−3.25±0.01	1.97±0.02	1.91±0.01
CdG1-6	1.45±0.005	1.31±0.01	−1.90±0.005	−1.75±0.01	−6.02±0.01	−2.96±0.01	3.06±0.02	3.30±0.01

[a] Scan rate: 100 mV s^{-1}; working electrode: Pt disc; auxiliary electrode: Pt wire; reference electrode: $Ag/AgNO_3$ in DMF; supporting electrolyte: Bu_4NPF_6 (0.1 M, DMF).

result from steric hindrance effects.[23] From the measured $E_{ox(onset)}$ values, the energies (in eV) of the corresponding highest occupied molecular orbital (HOMO) can be calculated according to Equation (1).

$$E_{HOMO} = -e(E_{ox(onset)} + 4.71) \quad (1)$$

$E_{ox(onset)}$ is the onset of oxidation potential versus Ag/$AgNO_3$.[24] Similarly, the energy (in eV) of the lowest unoccupied molecular orbital can be estimated from the value of $E_{red(onset)}$ by means of Equation (2).

$$E_{LUMO} = -e(E_{red(onset)} + 4.71) \quad (2)$$

The electrochemical band gap $E_{g(cv)}$, calculated by subtracting the HOMO from LUMO energy, is somewhat different from the corresponding optical band gap, $E_{g(opt)}$, because the states probed in the electrochemical experiments (free ions) and the optical measurements (neutral excited states) are different.[25]

As mentioned above, coordinatively bound self-assemblies carrying neutral ligands are ionized to intact supramolecular ions by removal of one or more of their counterions.[12] ESI MS of these Fe^{II} complexes led to supramolecular ions missing 4–10 PF_6^- counterions, hence having 4–10 positive charges, all of which were subjected to ion-mobility separation (Figure 2 and Figures S2–S6 in the Supporting Information). Because of the higher thermodynamic stability of ⟨tpy-Fe^{II}-tpy⟩, as compared to ⟨tpy-Cd^{II}-tpy⟩ bonds, ESI MS could be optimized to observe only the cyclic architectures after ion-mobility separation (vide infra and Figure 2 and Figure S2 in the Supporting Information). Note that both cyclic and ring-opened isomers were previously detected in less stable complexes[15a,c,e] as well as by Bowers et al.[15d] (see also Figure S7 in the Supporting Information).

The drift times of charge states formed by the Fe^{II} macrocycles can be obtained from the two-dimensional ESI-TWIM MS plots shown in Figure 2 and Figures S2–S6 (see Supporting Information). Calibration of the drift timescale with standards of known collision cross section makes it possible to convert these times into experimental cross-sectional areas.[14] Our calibration curve, established by the procedure of Scrivens et al.[14e] using protein standards, is depicted in Figure S8 in the Supporting Information; this curve could be used for all drift times >1.5 ms to derive the corresponding collision cross sections, which are listed in Table 3. For example, the ESI-TWIM MS plot in Figure S3 (Supporting Information) reveals that the $[M-4PF_6]^{4+}$, $[M-5PF_6]^{5+}$, $[M-6PF_6]^{6+}$, and $[M-7PF_6]^{7+}$ ions from **G1-6** have drift times of 4.06, 2.98, 2.53, and 1.71 ms, respectively. The collision cross sections deduced from these drift times using the calibration curve of Figure S8 (Supporting Information) are 1016.5, 1152.2, 1303.6, and 1246.5 Å^2 for $[M-4PF_6]^{4+}$ to $[M-7PF_6]^{7+}$, respectively. The cross sections are found to depend on the charge state of the macrocycle, that is, the number of PF_6^- counterions. A similar trend is observed for all other Fe^{II} macrocycles (Table 3). This result is different from a recent study by Bowers et al. on small, rigid, triangular and rectangular self-assemblies, for which no dependency of the collision cross section on the overall supramolecular ion charge was detected.[15d] Our finding is ascribed to the dendrons attached to the macrocycles; their branches can interact with each other, the PF_6^- counterions, and the aromatic moieties of the macrocycles, giving rise to many different conformers. Since the number of PF_6^- units influences the noncovalent interactions developed in the complexes, it also influences the number of conformers possible and the average collision cross section of these conformers, which is probed in the TWIM MS experiments.

Table 3. Experimental collision cross sections and modeled results of metallomacrocycles.

	Charge state	Drift times [ms]	Cross section (exptl) [Å^2]	Cross section (exptl av) [Å^2]	Cross section (calcd. av) [Å^2]
G1-5	+4	3.43	966.6	1026.6	985.1
	+5	2.53	1086.7		
	+6	1.62	1026.6		
G1-6	+4	4.06	1016.5	1179.7	1147.1
	+5	2.98	1152.2		
	+6	2.53	1303.6		
	+7	1.71	1246.5		
G1-7	+5	4.24	1287.3	1391.9	1317.8
	+6	2.89	1368.1		
	+7	2.53	1520.4		
G2-5	+5	4.15	1277.1	1410.2	1402.7
	+6	2.98	1379.7		
	+7	2.35	1469.8		
	+8	1.90	1514.2		
G2-6	+6	3.97	1512.0	1716.9	1692.3
	+7	3.07	1625.0		
	+8	2.89	1820.9		
	+9	2.26	1857.9		
	+10	1.71	1768.8		

The existence of a large number of conformers for each macrocyclic assembly is also indicated by the molecular mechanics/dynamics calculations. Geometry optimization of the Fe^{II} macrocycles by annealing simulations leads to structures falling within a wide range of collision cross sections, as attested by Figure S9–S13 (see Supporting Information), which depict the cross section versus relative energy span for 100 candidate structures from each Fe^{II} macrocycle. The average calculated cross sections of these complexes are included in Table 3 and agree very well with the corresponding average experimental cross sections (within 1–5%). Note that the counterions were not considered in the calculations; however, this does not cause any significant discrepancy between average calculated and experimental cross sections, pointing out that the contribution of the PF_6^- units to the overall collision cross-sectional area is negligibly small. The number of PF_6^- counterions appears to promote the formation of certain conformations, but the conformational space covered by all different charge states is quite similar to the family of conformers possible for the self-assembly without any counterions.

Both experimental and calculated collision cross sections gradually increase from pentamer **G1-5** to hexamer **G1-6** to

heptamer **G1-7**, which is consistent with the concomitant increase in the corresponding ring sizes. Cross sections also increase from **G1-5/6** to **G2-5/6** due to the higher generation of appended dendrons. Such results indicate that cross-sectional data can provide valuable information about molecular size and structure, benefitting this way the structural identification of similar compounds having different molecular sizes.

Conclusion

A family of well-defined macrocycles possessing ⟨tpy-Fe^{II}-tpy⟩ connectivity, ranging from pentamer to heptamer, and a ⟨tpy-Cd^{II}-tpy⟩-connected hexameric analogue, has been prepared using first- and second-generation, dendron-functionalized bis(terpyridine) ligands in a one-pot, self-assembly procedure. The resulting products were purified by column chromatography and their molecular structures as well as sizes were elucidated by NMR spectroscopy and ESI-TWIM MS. The high-resolution ^{1}H NMR spectra contained signals diagnostic for the respective ring size. The TWIM MS experiments provided evidence for the existence of several conformations for each macrocycle. The average collision cross sections of these conformers consistently increased with ring size and generation of dendrons attached to the macrocycles. Counterions did not significantly contribute to the molecular size of the assemblies, but promoted the generation of specific conformers. The photochemical and electrochemical properties of the complexes were significantly modulated by ring size, dendron generation of functionalized ligands, and metal ion center. Finally, it should be noted that the synthetic strategy presented here allows further functionalization at the periphery of the dendrons. For example, conversion of the *tert*-butyl ester to carboxylic acid groups would improve the water solubility of the macrocycles and remove the need for external counter-anions. Related work and further modification of these structures are ongoing.

Experimental Section

General procedures: Chemicals were commercially purchased and used without further purification. Thin-layer chromatography (TLC) was conducted on flexible sheets (Baker-flex) precoated with Al_2O_3 (IB-F) or SiO_2 (IB2-F) and the separated products were visualized by UV light. Column chromatography was conducted using basic Al_2O_3, Brockman Activity I (60–325 mesh) or SiO_2 (60–200 mesh) from Fisher Scientific. ^{1}H and ^{13}C NMR spectra were recorded on a Varian NMRS 500 spectrometer using $CDCl_3$, except where noted. UV/Vis spectra were recorded on a Perkin–Elmer Lambda 35 UV/Vis spectrometer. PL spectra were carried out on Perkin–Elmer LS55 luminescence spectrometer. Cyclic voltammetry was performed using a BASi EC epsilon workstation; scan rate: 100 mV s^{-1}; working electrode: Pt disc; auxiliary electrode: Pt wire; reference electrode: Ag/$AgNO_3$; supporting electrolyte: Bu_4NPF_6 (0.1 M, DMF). ESI mass spectra were obtained on a Bruker Esquire quadrupole ion trap mass spectrometer (ESI MS) or Waters Synapt HDMS quadrupole/time-of-flight (Q/ToF) tandem mass spectrometer (MS). MALDI-ToF MS measurements were performed with a Bruker UltraFlex III ToF/ToF MS, equipped with a Nd:YAG laser emitting at a wavelength of 355 nm. The proteins used to calibrate the drift time scale in traveling-wave ion-mobility mass spectrometry (TWIM MS) experiments, in order to obtain absolute collision cross sections, were acquired from Sigma–Aldrich. The TWIM MS experiments were performed using the following parameters: ESI capillary voltage: 1.0 kV; sample cone voltage: 7 V; extraction cone voltage: 3.2 V; desolvation gas flow: 800 L h^{-1} (N_2); trap collision energy (CE): 1 eV; transfer CE: 1 eV; trap gas flow: 1.5 mL min^{-1} (Ar); ion-mobility cell gas flow: 22.7 mL min^{-1} (N_2); sample flow rate: 5 μL min^{-1}; source temperature: 30 °C; desolvation temperature: 40 °C; IM traveling-wave height: 12 V or 8.5 V; and IM traveling-wave velocity: 350 m s^{-1}. The sprayed solution was prepared by dissolving the sample (≈0.3 mg) in a mixture of MeCN/MeOH (1 mL; 1:1, v/v). Data analyses were conducted using the MassLynx 4.1 and DriftScope 2.1 programs provided by Waters. Theoretical collision cross sections were calculated with the DriftScope 2.1 software.

Collision cross-section calibration: The drift timescale of the TWIM MS experiments was converted to a collision cross-section scale, following the calibration procedure of Scrivens et al.[14e] Briefly, the corrected collision cross sections of the molecular ions of insulin (bovine pancreas), ubiquitin (bovine red blood cells), and cytochrome C (horse heart), obtained from published work,[26,27] were plotted against the corrected drift times (arrival times) of the corresponding molecular ions measured in TWIM MS experiments at the same traveling-wave velocity, traveling-wave height, and ion-mobility gas flow setting used for the metallomacrocycles, namely, 350 m s^{-1}, 12 V, and 22.7 mL min^{-1}, respectively. All charge states observed for the calibrants were used in the construction of the curve.

Molecular modeling: Energy minimization of the macrocycles was conducted with the Materials Studio version 4.2 program, using the Anneal and Geometry Optimization tasks in the Forcite module (Accelrys Software, Inc.). The counterions were omitted. An initially energy-minimized structure was subjected to 100 anneal cycles with initial and mid-cycle temperatures of 300 and 1400 K, respectively, twenty heating ramps per cycle, one thousand dynamics steps per ramp, and one dynamics step per femtosecond. A constant volume/constant energy (NVE) ensemble was used; the geometry was optimized after each cycle. All geometry optimizations used a universal force field with atom-based summation and cubic spline truncation for both the electrostatic and van der Waals parameters. For each macrocycle, 100 candidate structures were generated for the calculation of collision cross sections (see Supporting Information).

Synthesis of G1tpy: **G1tpy** was prepared (82%) according to literature[16] from the free amine of bis(terpyridine) **1** and the Newkome-type, first-generation dendron **2**.

Synthesis of G2tpy: A stirred mixture of the isocyanate of dendron **3** (270 mg, 184 μmol) and free amine of bis(terpyridine)[16] **1** (100 mg, 163 μmol) in $CHCl_3$ (30 mL) was maintained at 25 °C for 10 h; after removal of the solvent in vacuo the residue was purified by column chromatography (Al_2O_3, $CHCl_3$/MeOH, 95:5) to afford **G2tpy**, as a white solid (242 mg, 72%). M.p. 88–90 °C; ^{1}H NMR ($CDCl_3$, 500 MHz): δ = 8.76 (s, 4H; Py$H^{3',5'}$), 8.70–8.71 (d, J = 4.5 Hz, 4H; Py$H^{6,6''}$), 8.64–8.66 (d, J = 8.0 Hz, 4H; Py$H^{3,3''}$), 7.84–7.88 (m, 5H; Ph-H, Py$H^{4,4''}$), 7.46 (d, J = 1.5 Hz, 2H; PhH), 7.32–7.34 (m, 4H; Py$H^{5,5''}$), 6.15 (s, 1H; NH), 6.11 (s, 3H; NH), 4.99–5.01 (t, J = 5.5 Hz, 1H; NH), 4.25–4.28 (m, J = 5.5 Hz, 2H; OCH_2), 3.40–3.44 (m, 2H; NCH_2), 2.09–2.23 (m, 26H; CH_2), 1.94–2.00 (m, 24H; CH_2), 1.42 ppm (s, 81H; CH_3); ^{13}C NMR ($CDCl_3$, 125 MHz): δ = 173.3, 172.9, 160.2, 158.2, 156.4, 156.2, 150.4, 149.3, 141.1, 136.9, 123.9, 121.5, 119.5, 119.0, 114.4, 80.7, 66.4, 57.5, 56.9, 37.7, 32.9, 32.1, 30.6, 30.0, 28.2; MALDI-ToF MS: m/z calcd for $C_{116}H_{163}N_{11}O_{23}$: 2078.2; found: 2100.5 $[M+Na]^+$.

Synthesis of G1-5, G1-6, and G1-7: A solution of $FeCl_2 \cdot 4H_2O$ (21 mg, 0.11 mmol) in MeOH (200 mL) was added to a stirred solution of **G1tpy** (105 mg, 100 μmol) in MeOH (200 mL). After stirring the mixture at 25 °C for 10 h, the purple solution was concentrated in vacuo to give a residue, which was purified by flash column chromatography (SiO_2) using H_2O/MeCN/sat.KNO_3(aq), as the mobile phase to successively elute **G1-5** (solvent composition, 1:12:1 v/v/v), **G1-6** (1:10:1), and **G1-7** (1:8:1),

which were isolated as purple solids. Multiple column chromatograph separations were necessary to obtain the pure compounds, resulting in relatively low overall yields.

Data for ***G1-5***: Yield: 11.3 mg, 8%; ^{1}H NMR (CD_3OD, 500 MHz): $\delta=$ 9.64 (s, 20H; Py$H^{3',5'}$), 8.95–8.96 (d, $J=7.5$ Hz, 20H; Py$H^{3,3''}$), 8.75 (s, 5H; PhH), 8.22 (s, 10H; PhH), 7.96–7.99 (m, 20H; Py$H^{4,4''}$), 7.38–7.39 (d, $J=$ 5.0 Hz, 20H; Py$H^{6,6''}$), 7.20–7.22 (m, 20H; Py$H^{5,5''}$), 4.57–4.60 (m, 10H; OCH_2), 3.53–3.55 (t, $J=6.3$ Hz, 10H; NCH_2), 2.25–2.28 (m, 40H; CH_2), 1.94–1.98 (m, 30H; CH_2), 1.42 ppm (s, 135H; CH_3); ^{13}C NMR (CD_3OD, 125 MHz): $\delta=$174.8, 162.8, 162.2, 160.1, 159.9, 154.3, 153.4, 141.6, 140.3, 128.9, 125.7, 123.9, 123.2, 117.0, 81.8, 68.4, 57.6, 37.9, 31.8, 31.5, 30.9, 28.5 ppm; ESI MS: m/z: 1606.7 $[M-4PF_6^-]^{4+}$ (calcd m/z: 1606.3), 1256.4 $[M-5PF_6^-]^{5+}$ (calcd m/z: 1256.0), 1022.8 $[M-6PF_6^-]^{6+}$ (calcd m/z: 1022.5), 855.9 $[M-7PF_6^-]^{7+}$ (calcd m/z: 855.7), 730.8 $[M-8PF_6^-]^{8+}$ (calcd m/z: 730.7), 633.5 $[M-9PF_6^-]^{9+}$ (calcd m/z: 633.4), 555.7 $[M-10PF_6^-]^{10+}$ (calcd m/z: 555.5).

Data for ***G1-6***: Yield: 29.1 mg, 21%; ^{1}H NMR (CD_3OD, 500 MHz): $\delta=$ 9.70 (s, 24H; Py$H^{3',5'}$), 8.98–8.99 (d, $J=8.0$ Hz, 24H; Py$H^{3,3''}$), 8.94 (s, 6H; PhH), 8.26 (s, 12H; PhH), 7.98–8.01 (m, 24H; Py$H^{4,4''}$), 7.42–7.43 (d, $J=$ 5.5 Hz, 24H; Py$H^{6,6''}$), 7.22–7.24 (m, 24H; Py$H^{5,5''}$), 4.58–4.59 (s, $J=$ 6.0 Hz, 12H; OCH_2), 3.52–3.55 (t, $J=6.5$ Hz,12H; NCH_2), 2.24–2.27 (m, 48H; CH_2), 1.93–1.96 (m, 36H; CH_2), 1.42 ppm (s, 162H; CH_3); ^{13}C NMR (CD_3OD, 125 MHz): $\delta=$174.8, 162.8, 162.2, 160.1, 159.9, 154.3, 152.0, 141.3, 140.3, 129.0, 125.8, 123.6, 122.1, 117.4, 81.8, 68.5, 57.6, 37.9, 31.8, 31.5, 30.9, 28.5 ppm; ESI MS: m/z: 1957.2 $[M-4PF_6^-]^{4+}$ (calcd m/z:1956.6), 1536.8 $[M-5PF_6^-]^{5+}$ (calcd m/z: 1536.3), 1256.4 $[M-6PF_6^-]^{6+}$ (calcd m/z: 1256.1), 1056.1 $[M-7PF_6^-]^{7+}$ (calcd m/z: 1056.0), 905.9 $[M-8PF_6^-]^{8+}$ (calcd m/z: 905.8), 789.2 $[M-9PF_6^-]^{9+}$ (calcd m/z: 789.1), 695.8 $[M-10PF_6^-]^{10+}$ (calcd m/z: 695.7), 619.4 $[M-11PF_6^-]^{11+}$ (calcd m/z: 619.3), 555.7 $[M-12PF_6^-]^{12+}$ (calcd m/z: 555.6).

Data for ***G1-7***: Yield: 7.1 mg, 5%; ^{1}H NMR (CD_3OD, 500 MHz): $\delta=$ 9.73 (s, 28H; Py$H^{3',5'}$), 9.00–9.02 (d, $J=7.5$ Hz, 35H; Py$H^{3,3''}$), 8.28 (s, 14H; PhH), 7.99–8.02 (m, 28H; Py$H^{4,4''}$), 7.43–7.44 (d, $J=5.0$ Hz, 28H; Py$H^{6,6''}$), 7.23–7.25 (m, 24H; Py$H^{5,5''}$), 4.57–4.61 (m, 14H; OCH_2), 3.52–3.55 (t, $J=6.0$ Hz, 14H; NCH_2), 2.23–2.26 (m, 56H; CH_2), 1.92–1.95 (m, 42H; CH_2), 1.41 ppm (s, 189H; CH_3); ^{13}C NMR (CD_3OD, 125 MHz): $\delta=$ 174.8, 162.9, 162.2, 160.1, 159.9, 154.2, 151.9, 141.2, 140.4, 129.0, 125.9, 123.5, 121.7, 117.6, 81.8, 68.5, 57.6, 37.9, 31.9, 31.5, 30.9, 28.5 ppm; ESI MS: m/z: 1489.9 $[M-6PF_6^-]^{6+}$ (calcd m/z: 1489.7), 1256.5 $[M-7PF_6^-]^{7+}$ (calcd m/z: 1256.2), 1081.1 $[M-8PF_6^-]^{8+}$ (calcd m/z: 1081.0), 944.9 $[M-9PF_6^-]^{9+}$ (calcd m/z: 944.8), 835.9 $[M-10PF_6^-]^{10+}$ (calcd m/z: 835.8), 746.7 $[M-11PF_6^-]^{11+}$ (calcd m/z: 746.7), 672.4 $[M-12PF_6^-]^{12+}$ (calcd m/z: 672.4), 609.6 $[M-13PF_6^-]^{13+}$ (calcd m/z: 609.5).

Synthesis of G2-5 and G2-6: A solution of $FeCl_2{\cdot}4H_2O$ (11.5 mg, 58 μmol) in MeOH (200 mL) was added to a stirred solution of **G2tpy** (114 mg, 55 μmol) in MeOH (200 mL). After the mixture was stirred at 25°C for 10 h, the resultant purple solution was concentrated in vacuo to give a residue, which was purified by flash column chromatography (SiO_2) using H_2O/MeCN/sat. KNO_3(aq), as the mobile phase to successively elute **G2-5** with a 1:14:1 (v/v/v) mixture and **G2-6** with a 1:12:1 mixture. A column chromatography separation was repeated several times to obtain the pure compounds, which led to relatively low overall yields.

Data for ***G2-5***: Yield: 13.4 mg, 10%; ^{1}H NMR (CD_3OD, 500 MHz): $\delta=$ 9.72 (s, 20H; Py$H^{3',5'}$), 8.96–8.98 (d, $J=8.0$ Hz, 20H; Py$H^{3,3''}$), 8.70 (s, 5H; Ph-H), 8.22 (s, 10H; PhH), 7.96–7.99 (m, 20H; Py$H^{4,4''}$), 7.39–7.40 (d, $J=$ 5.1 Hz, 20H; Py$H^{6,6''}$), 7.21–7.23 (m, 20H; Py$H^{5,5''}$), 4.60 (m, 10H; OCH_2), 3.55 (m,10H; NCH_2), 2.18–2.25 (m, 130H; CH_2), 1.91–2.02 (m, 120H; CH_2), 1.42 ppm (s, 405H; CH_3); ^{13}C NMR (CD_3OD, 125 MHz): $\delta=$175.6, 174.6, 162.8, 162.2, 160.4, 159.9, 154.3, 152.4, 141.6, 140.3, 129.0, 125.8, 124.0, 123.1, 122.2, 117.1, 81.8, 68.5, 58.8, 57.9, 37.9, 33.3, 32.4, 32.1, 30.9, 30.7, 28.6 ppm; ESI MS: m/z: 2887.5 $[M-4PF_6^-]^{4+}$ (calcd m/z: 2286.4), 2280.8 $[M-5PF_6^-]^{5+}$ (calcd m/z: 2280.1), 1876.7 $[M-6PF_6^-]^{6+}$ (calcd m/z: 1875.9), 1587.7 $[M-7PF_6^-]^{7+}$ (calcd m/z: 1587.2), 1371.2 $[M-8PF_6^-]^{8+}$ (calcd m/z: 1370.7), 1202.7 $[M-9PF_6^-]^{9+}$ (calcd m/z: 1202.3).

Data for ***G2-6***: Yield: 31 mg, 23%; ^{1}H NMR (CD_3OD, 500 MHz): $\delta=$ 9.77 (s, 24H; Py$H^{3',5'}$), 9.00–9.02 (d, $J=7.5$ Hz, 24H; Py$H^{3,3''}$), 8.91 (s, 6H; PhH), 8.26 (s, 12H; PhH), 7.99–8.02 (m, 24H; Py$H^{4,4''}$), 7.42–7.43 (d, $J=$ 5.0 Hz, 24H; Py$H^{6,6''}$), 7.23–7.25 (m, 24H; Py$H^{5,5''}$), 4.60 (m, 12H; OCH_2), 3.54 (m,12H; NCH_2), 2.18–2.21 (m, 156H; CH_2), 1.92–2.04 (m, 144H; CH_2), 1.41 ppm (s, 486H; CH_3); ^{13}C NMR (CD_3OD, 125 MHz): $\delta=$175.6, 174.6, 162.8, 162.2, 160.4, 159.9, 154.3, 152.1, 141.3, 140.4, 129.1, 125.9, 123.7, 121.9, 117.5, 81.8, 68.5, 58.8, 57.9, 38.0, 33.3, 32.7, 32.4, 30.9, 30.7, 28.6 ppm; ESI MS: m/z: 2766.1 $[M-5PF_6^-]^{5+}$ (calcd m/z: 2764.9), 2280.8 $[M-6PF_6^-]^{6+}$ (calcd m/z: 2279.9), 1934.1 $[M-7PF_6^-]^{7+}$ (calcd m/z: 1933.5), 1674.3 $[M-8PF_6^-]^{8+}$ (calcd m/z: 1673.7), 1472.2 $[M-9PF_6^-]^{9+}$ (calcd m/z: 1471.6), 1310.5 $[M-10PF_6^-]^{10+}$ (calcd m/z: 1310.0), 1178.2 $[M-11PF_6^-]^{11+}$ (calcd m/z: 1177.7).

Synthesis of CdG1-6: A solution of $Cd(NO_3)_2{\cdot}4H_2O$ (12 mg, 38 μmol) in MeOH (5 mL) was added to a solution of ligand **G1tpy** (40 mg, 38 μmol) in MeOH (10 mL). The mixture was stirred at 25°C for 1 h. After removal of solvent in vacuo, white solid was generated. And then dissolved in MeOH, and excess NH_4PF_6 was added to generate a white precipitate, which was washed with MeOH and water to give the desire **CdG1-6** possessing PF_6^-, as the counterions (52 mg, 94%). ^{1}H NMR (CD_3CN, 500 MHz): $\delta=$9.15 (s, 24H; Py$H^{3',5'}$), 8.90–8.92 (d, $J=6.9$ Hz, 24H; Py$H^{3,3''}$), 8.44 (s, 6H; PhH), 8.18–8.28 (m, 48H; Py$H^{4,4''}$, Py$H^{6,6''}$), 7.99 (s, 12H; PhH), 7.57 (m, 24H; Py$H^{5,5''}$), 4.99–5.03 (t, $J=5.7$ Hz, 6H; CONH), 4.65 (s, 6H; CONH), 4.47 (m, 12H; OCH_2), 3.40–3.42 (m, 12H; NCH_2), 2.18 (m, 48H; CH_2), 1.82–1.88 (m, 36H; CH_2), 1.38 ppm (s, 162H; CH_3); ^{13}C NMR (CD_3CN, 125 MHz): $\delta=$174.1, 162.3, 158.5, 155.9, 151.9, 151.2, 150.2, 142.8, 140.6, 128.9, 125.3, 123.8,121.2, 117.9, 81.2, 68.5, 57.5, 38.1, 31.7, 31.4, 30.9, 28.7; ESI MS: m/z: 2771.2 $[M-3PF_6^-]^{3+}$ (calcd m/z: 2770.1), 2042.2 $[M-4PF_6^-]^{4+}$ (calcd m/z: 2041.3), 1604.6 $[M-5PF_6^-]^{5+}$ (calcd m/z:1604.1), 1312.8 $[M-6PF_6^-]^{6+}$ (calcd m/z: 1312.6), 1104.7 $[M-7PF_6^-]^{7+}$ (calcd m/z:1104.4).

Acknowledgements

The authors gratefully thank the National Science Foundation (DMR-0812337 and DMR-0705015 to G.R.N.; CHE-1012636 and DMR-0821313 to C.W.) and the Ohio Board of Regents for financial support.

[1] a) J.-M. Lehn, *Supramolecular Chemistry: Concepts and Perspectives*, VCH, Weinheim, **1995**; b) D. Philp, J. F. Stoddart, *Angew. Chem.* **1996**, *108*, 1242–1286; *Angew. Chem. Int. Ed. Engl.* **1996**, *35*, 1154–1196; c) P. J. Stang, N. E. Persky, J. Manna, *J. Am. Chem. Soc.* **1997**, *119*, 4777–4778; d) S. Leininger, B. Olenyuk, P. J. Stang, *Chem. Rev.* **2000**, *100*, 853–908; e) B. J. Holliday, C. A. Mirkin, *Angew. Chem.* **2001**, *113*, 2076–2097; *Angew. Chem. Int. Ed.* **2001**, *40*, 2022–2043; f) J.-M. Lehn, *Science* **2002**, *295*, 2400–2403; g) G. M. Whitesides, B. Grzybowski, *Science* **2002**, *295*, 2418–2421; h) B. H. Northrop, Y. R. Zheng, K. W. Chi, P. J. Stang, *Acc. Chem. Res.* **2009**, *42*, 1554–1563.

[2] a) G. S. Hanan, D. Volkmer, U. S. Schubert, J.-M. Lehn, G. Baum, D. Fenske, *Angew. Chem.* **1997**, *109*, 1929–1931; *Angew. Chem. Int. Ed. Engl.* **1997**, *36*, 1842–1844; b) T. E. Janini, J. L. Fattore, D. L. Mohler, *J. Organomet. Chem.* **1999**, *578*, 260–263; c) T. Bark, M. Düggeli, H. Stoeckli-Evans, A. von Zelewsky, *Angew. Chem.* **2001**, *113*, 2924–2927; *Angew. Chem. Int. Ed.* **2001**, *40*, 2848–2851.

[3] a) M. Fujita, J. Yazaki, K. Ogura, *J. Am. Chem. Soc.* **1990**, *112*, 5645–5647; b) M. Fujita, M. Tominaga, A. Hori, B. Therrien, *Acc. Chem. Res.* **2005**, *38*, 369–380; c) M. Yoshizawa, J. K. Klosterman, M. Fujita, *Angew. Chem.* **2009**, *121*, 3470–3490; *Angew. Chem. Int. Ed.* **2009**, *48*, 3418–3438; d) Q. F. Sun, J. Iwasa, D. Ogawa, Y. Ishido, S. Sato, T. Ozeki, Y. Sei, K. Yamaguchi, M. Fujita, *Science* **2010**, *328*, 1144–1147.

[4] a) X. Liu, C. L. Stern, C. A. Mirkin, *Organometallics* **2002**, *21*, 1017–1019; b) N. C. Gianneschi, M. S. Masar, C. A. Mirkin, *Acc. Chem. Res.* **2005**, *38*, 825–837; c) C. G. Oliveri, P. A. Ulmann, M. J. Wiester, C. A. Mirkin, *Acc. Chem. Res.* **2008**, *41*, 1618–1629.

[5] a) A. Kumar, S. S. Sun, A. J. Lees, *Coord. Chem. Rev.* **2008**, *252*, 922–939; b) E. C. Constable, *Coord. Chem. Rev.* **2008**, *252*, 842–855; c) S. J. Lee, W. Lin, *Acc. Chem. Res.* **2008**, *41*, 521–537.

[6] a) M. M. Ali, F. M. MacDonnell, *J. Am. Chem. Soc.* **2000**, *122*, 11527–11528; b) F. A. Cotton, L. M. Daniels, C. Lin, C. A. Murillo, S.-Y. Yu, *J. Chem. Soc. Dalton Trans.* **2001**, 502–504; c) M. Schweiger, S. R. Seidel, A. M. Arif, P. J. Stang, *Angew. Chem.* **2001**, *113*, 3575–3577; *Angew. Chem. Int. Ed.* **2001**, *40*, 3467–3469; d) F. A. Cotton, C. Lin, C. A. Murillo, *J. Am. Chem. Soc.* **2001**, *123*, 2670–2671; e) S. J. Lee, A. Hu, W. Lin, *J. Am. Chem. Soc.* **2002**, *124*, 12948–12949; f) G. R. Newkome, T. J. Cho, C. N. Moorefield, R. Cush, P. S. Russo, L. A. Godínez, M. J. Saunders, P. Mohapatra, *Chem. Eur. J.* **2002**, *8*, 2946–2954; g) Y. K. Kryschenko, S. R. Seidel, A. M. Arif, P. J. Stang, *J. Am. Chem. Soc.* **2003**, *125*, 5193–5198; h) S. R. Halper, S. M. Cohen, *Angew. Chem.* **2004**, *116*, 2439–2442; *Angew. Chem. Int. Ed.* **2004**, *43*, 2385–2388; i) X.-C. Huang, J.-P. Zhang, X.-M. Chen, *J. Am. Chem. Soc.* **2004**, *126*, 13218–13219; <*lit* j> T. Megyes, H. Jude, T. Grosz, I. Bako, T. Radnai, G. Tarkanyi, G. Palinkas, P. J. Stang, *J. Am. Chem. Soc.* **2005**, *127*, 10731–10738; k) E. Zangrando, M. Casanova, E. Alessio, *Chem. Rev.* **2008**, *108*, 4979–5013; l) S. Ghosh, P. S. Mukherjee, *Inorg. Chem.* **2009**, *48*, 2605–2613; <*lit* m> Y.-T. Chan, C. N. Moorefield, M. Soler, G. R. Newkome, *Chem. Eur. J.* **2010**, *16*, 1768–1771.

[7] a) D. Armspach, M. Cattalini, E. C. Constable, C. E. Housecroft, D. Phillips, *Chem. Commun.* **1996**, 1823–1824; b) E. C. Constable, *Chem. Commun.* **1997**, 1073–1080; c) G. R. Newkome, T. J. Cho, C. N. Moorefield, G. R. Baker, M. J. Saunders, R. Cush, P. S. Russo, *Angew. Chem.* **1999**, *111*, 3899–3903; *Angew. Chem. Int. Ed.* **1999**, *38*, 3717–3721; d) H. Hofmeier, U. S. Schubert, *Chem. Soc. Rev.* **2004**, *33*, 373–399; e) G. R. Newkome, T. J. Cho, C. N. Moorefield, P. P. Mohapatra, L. A. Godínez, *Chem. Eur. J.* **2004**, *10*, 1493–1500; f) U. S. Schubert, H. Hofmeier, G. R. Newkome, *Modern Terpyridine Chemistry*, Wiley-VCH, Weinheim, **2006**; g) S.-H. Hwang, P. Wang, C. N. Moorefield, L. A. Godinez, J. Manriquez, E. Bustos, G. R. Newkome, *Chem. Commun.* **2005**, 4672–4674.

[8] a) G. R. Newkome, C. Shreiner, *Chem. Rev.* **2010**, *110*, 6338–6442; b) D. Astruc, E. Boisselier, C. Ornelas, *Chem. Rev.* **2010**, *110*, 1857–1959; c) N. Sakai, Y. Kamikawa, M. Nishii, T. Matsuoka, T. Kato, S. Matile, *J. Am. Chem. Soc.* **2006**, *128*, 2218–2219.

[9] a) B. Grossmann, J. Heinze, E. Herdtweck, H. Noth, M. Schwenk, W. Wachter, W. Weber, *Angew. Chem.* **1997**, *109*, 384–386; *Angew. Chem. Int. Ed. Engl.* **1997**, *36*, 387–389; b) E. C. Constable, C. E. Housecroft, M. Neuburger, S. Schaffner, L. J. Scherer, *Dalton Trans.* **2004**, 2635–2642; c) R. Takahashi, Y. Kobuke, *J. Am. Chem. Soc.* **2003**, *125*, 2372–2373; d) O. Shoji, S. Okada, A. Satake, Y. Kobuke, *J. Am. Chem. Soc.* **2005**, *127*, 2201–2210; e) H.-B. Yang, N. Das, F. Huang, A M. Hawkridge, D. C. Muddiman, P. J. Stang, *J. Am. Chem. Soc.* **2006**, *128*, 10014–10015; f) X.-D. Xu, H.-B. Yang, Y.-R. Zheng, K. Ghosh, M. M. Lyndon, D. C. Muddiman, P. J. Stang, *J. Org. Chem.* **2010**, *75*, 7373–7380; g) G.-Z. Zhao, L.-J. Chen, C.-H. Wang, H.-B. Yang, K. Ghosh, Y.-R. Zheng, M. M. Lyndon, D. C. Muddiman, P. J. Stang, *Organometallics* **2010**, *29*, 6137–6140; h) T. Chen, G.-B. Pan, H. Wettach, M. Fritzsche, S. Hoger, L.-J. Wan, H.-B. Yang, B. H. Northrop, P. J. Stang, *J. Am. Chem. Soc.* **2010**, *132*, 1328–1333.

[10] a) S. Sato, Y. Ishido, M. Fujita, *J. Am. Chem. Soc.* **2009**, *131*, 6064–6065; b) W. Jiang, A. Schafer, P. C. Mohr, C. A. Schalley, *J. Am. Chem. Soc.* **2010**, *132*, 2309–2320.

[11] a) H. Jiang, W. Lin, *J. Am. Chem. Soc.* **2004**, *126*, 7426–7427; b) H. Jiang, W. Lin, *J. Am. Chem. Soc.* **2006**, *128*, 11286–11297.

[12] P. Wang, G. R. Newkome, C. Wesdemiotis, *Int. J. Mass Spectrom.* **2006**, *255–256*, 86–92.

[13] a) M. T. Bowers, P. R. Kemper, von G. Helden, van P. A. M. Koppen, *Science* **1993**, *260*, 1446–1451; b) C. S. Hoaglund-Hyzer, A. E. Counterman, D. E. Clemmer, *Chem. Rev.* **1999**, *99*, 3037–3079; c) G. F. Verbeck, B. T. Ruotolo, H. A. Sawyer, K. J. Gillig, D. H. Russell, *J. Biomol. Technol.* **2002**, *13*, 56–61; d) S. Trimpin, D. I. Plasencia, D. E. Clemmer, *Anal. Chem.* **2007**, *79*, 7965–7974; e) S. Trimpin, D. E. Clemmer, *Anal. Chem.* **2008**, *80*, 9073–9083; f) A. P. Gies, M. Kliman, J. A. McLean, D. M. Hercules, *Macromolecules* **2008**, *41*, 8299–9301.

[14] a) B. T. Ruotolo, J. L. P. Benesch, A. M. Sandercock, S. J. Hyung, C. V. Robinson, *Nature Protocols* **2008**, *3*, 1139–1152; b) C. Uetrecht, C. Versluis, N. R. Watts, P. T. Wingfield, A. C. Steven, A. J. R. Heck, *Angew. Chem.* **2008**, *120*, 6343–6347; *Angew. Chem. Int. Ed.* **2008**, *47*, 6247–6251; c) E. Van Duijn, A. Barendregt, S. Synowsky, C. Versluis, A. J. R. Heck, *J. Am. Chem. Soc.* **2009**, *131*, 1452–1459; d) A. C. Joerger, S. Rajagopalan, E. Natan, D. B. Veprintsev, C. V. Robinson, A. R. Fersht, *Proc. Natl. Acad. Sci. USA* **2009**, *106*, 17705–17710; e) K. Thalassinos, M. Grabenauer, S. E. Slade, G. R. Hilton, M. T. Bowers, J. H. Scrivens, *Anal. Chem.* **2009**, *81*, 248–254; f) D. P. Smith, W. W. Knapman, I. Campuzano, R. W. Malham, J. T. Berryman, S. E. Radford, A. E. Ashcroft, *Eur. J. Mass Spectrom.* **2009**, *15*, 113–130.

[15] a) Y.-T. Chan, X. Li, M. Soler, J. L. Wang, C. Wesdemiotis, G. R. Newkome, *J. Am. Chem. Soc.* **2009**, *131*, 16395–16397; b) X. Ren, B. Sun, C.-C. Tsai, Y. Tu, S. Leng, K. Li, Z. Kang, R. M. Van Horn, X. Li, M. Zhu, C. Wesdemiotis, W.-B. Zhang, S. Z. D. Cheng, *J. Phys. Chem. B* **2010**, *114*, 4802–4810; c) S. Perera, X. Li, M. Soler, A. Schultz, C. Wesdemiotis, C. N. Moorefield, G. R. Newkome, *Angew. Chem.* **2010**, *122*, 6689–6694; *Angew. Chem. Int. Ed.* **2010**, *49*, 6539–6544; d) E. R. Brocker, S. E. Anderson, B. H. Northrop, P. J. Stang, M. T. Bowers, *J. Am. Chem. Soc.* **2010**, *132*, 13486–13494; e) Y.-T. Chan, X. Li, C. N. Moorefield, C. Wesdemiotis, G. R. Newkome, *J. Am. Chem. Soc.* submitted; f) X. Li, Y.-T. Chan, G. R. Newkome, C. Wesdemiotis, *Anal. Chem.* **2011**, *83*, 1284–1290.

[16] P. Wang, C. N. Moorefield, G. R. Newkome, *Org. Lett.* **2004**, *6*, 1197–1200.

[17] G. R. Newkome, E. He, L. A. Godínez, *Macromolecules* **1998**, *31*, 4382–4386.

[18] P. S. Braterman, J.-I. Song, R. D. Peacock, *Inorg. Chem.* **1992**, *31*, 555–559.

[19] X. Chen, Y. Ding, Y. Cheng, L. Wang, *Synth. Met.* **2010**, *160*, 625–630.

[20] a) J. Pei, J.-L. Wang, X.-Y. Cao, X.-H. Zhou, W.-B. Zhang, *J. Am. Chem. Soc.* **2003**, *125*, 9944–9945; b) J.-L. Wang, J. Yan, Z.-M. Tang, Q. Xiao, Y. Ma, J. Pei, *J. Am. Chem. Soc.* **2008**, *130*, 9952–9962.

[21] J. K. McCusker, K. N. Walda, R. C. Dunn, J. D. Simon, D. Magde, D. N. Hendrickson, *J. Am. Chem. Soc.* **1993**, *115*, 298–307.

[22] H.-F. Chow, I. Y. K. Chan, D. T. Chan, R. W. Kwok, *Chem. Eur. J.* **1996**, *2*, 1085–1091.

[23] G. R. Newkome, R. Güther, C. N. Moorefield, F. Cardullo, L. Echegoyen, E. Pérez-Cordero, H. Luftmann, *Angew. Chem.* **1995**, *107*, 2159–2162; *Angew. Chem. Int. Ed. Engl.* **1995**, *34*, 2023–2026.

[24] Q. Sun, H. Wang, C. Yang, Y. Li, *J. Mater. Chem.* **2003**, *13*, 800–806.

[25] C.-Q. Ma, M. Fonrodona, M. C. Schikora, M. M. Wienk, R. A. J. Janssen, P. Bäuerle, *Adv. Funct. Mater.* **2008**, *18*, 3323–3331.

[26] F. A. Fernandez-Lima, R. C. Blasé, D. H. Russell, *Int. J. Mass Spectrom.* **2010**, *298*, 111–118.

[27] http://www.indiana.edu/~clemmer/Research/cross%20section%20database/Proteins/protein cs.htm.

Received: December 20, 2010
Published online: March 21, 2011

